

Grain-boundary effect in calcium thin films

P. Renucci, L. Gaudart, J. P. Petrakian, and D. Roux

Centre d'Etude des Couches Minces, Laboratoire associé au Centre National de la Recherche Scientifique,

Faculté des Sciences et Techniques, 13397 Marseille Cedex 13, France

(Received 18 February 1981; revised manuscript received 9 April 1982)

Deposition and study of calcium films were achieved under ultrahigh vacuum. The latter was obtained with the use of an ion pump and a helium cryopump. The temperature of the substrate ranged between 90 and 400 K. The electrical resistance was measured with the use of a four-probe method with a constant current. Film thicknesses were in the range between 20 and 300 nm. To obtain a stable film structure, samples were annealed to a temperature near 400 K. The electrical resistivity of the annealed films exhibited a linear and reversible variation with temperature. It was shown to be thickness dependent. For the thickest deposits, electrical resistivity reached a constant value which no longer depended on the thickness, but was a function of the film-deposition temperature. With the help of electron photomicrographs and with use of the conduction model proposed by Mayadas and Schatzkes, we calculated the fraction p of electrons which are specularly reflected at the surface of the film and the parameter α depending on the reflection on grain boundaries. The influence of grain boundaries was calculated and the mean free path was deduced from these results.

I. INTRODUCTION

Polycrystalline thin films exhibit three kinds of electronic properties: bulk properties, properties that are induced by the surface, and properties that are connected with the crystal arrangement and the size of the aggregates. With alkaline-earth metals, very liable to deterioration, it is not possible to use direct electron micrograph techniques to investigate thin-film structures. Indeed, the study of such films has to be achieved *in situ*, under ultrahigh vacuum (UHV). Bulk properties as well as surface electronic energies can be obtained from optical or photoemission measurements,^{1,2} whereas the shape and the roughness of the surface are often studied using electron photomicrographs of carbon replicas, as shown by Rasigni *et al.*³ But none of these techniques gives information about the aggregates inside the film. The study of the electrical conductivity is a method to obtain some information about the structure of the bulk and to study transport phenomena. The thickness of the film is a convenient parameter, since electronic properties are thickness dependent. The electrons are scattered by the grain boundaries, and quantities like the mean free path or the reflection coefficient at the grain boundaries may give an idea of the film structure. Comparison

between optical and electrical properties^{4,5} enables us to obtain a better understanding of experimental results.

For calcium, optical properties were studied by Hunderi,⁶ Marfaing and Rivoira,⁷ and Nilsson and Forssell.⁸ Photoemission studies were performed by Gaudart and Rivoira⁹ and by Kress and Lapeyre.¹⁰ On the other hand, energy-band diagrams were calculated, in particular, by Mickish *et al.*¹¹ and Lopez-Rios and Sommers.¹² The electrical resistance behavior at high pressures and low temperatures has been studied recently by Dunn and Bundy.¹³ The essential purpose of this work is to study transport phenomena in calcium thin films.

From a technical point of view, the study of the alkaline-earth metals is difficult, because of their great affinity for oxygen and water vapor. Clean ultrahigh-vacuum conditions are needed to obtain unaltered thin films that must be studied *in situ*. Moreover, an annealing procedure is necessary to eliminate defects and to get stable film structure. In the final state, reversible changes in resistance of thin films are observed. This study concerns continuous thin films (i.e., films made up of a single material without holes), but our apparatus enables us to study also lacunar films, i.e., presenting holes. Data were compared with the Mayadas and Shatzkes theory.¹⁴

II. EXPERIMENTAL ARRANGEMENT

Thin calcium films were obtained and studied *in situ* at a pressure near 2×10^{-10} Torr. A particularly low pressure is very important as it is well known that an ordinary vacuum induces thin-film alterations and mechanical effects.¹⁵ Films were obtained by thermal evaporation and deposited onto a cooled silica substrate at a low rate (0.05 nm/s). The thickness of a deposit, which is evaporation-time dependent, was measured by means of the frequency variations of a quartz oscillator, and ranged from 20 to 300 nm. The amount of metal deposited on the substrate determines the structure of the film. Such films are usually polycrystalline.

The UHV system (Fig. 1) was composed of three parts: a pumping unit, an evaporating chamber, and a cell for measurements. It is difficult to obtain bulk alkaline-earth metals that have a high degree of purity. It ensues that when outgassing and during the thermal evaporation, a subsequent rise of the pressure in the chamber has to be expected. If a single ion pump was used, titanium plates would be rapidly contaminated by metallic vapor. In order to avoid this phenomenon, we combined a helium-cooled cryopump with an ion pump. Calcium ingots of 99.9% purity were preserved under ultrahigh vacuum in the evaporating chamber, which could be separated from the measurement cell by an ultrahigh-vacuum valve. The ingots were placed in

an aluminum oxide crucible that was heated by Joule effect. The distance between the vapor source and the substrate was about 50 cm. According to the previous work of Bondarenko and Makhov¹⁶ concerning the great importance of outgassing for barium, various outgassing had to be done for calcium. During the evaporation of the film, the pressure increases to 3×10^{-9} Torr in the cell and 5×10^{-8} Torr in the evaporating chamber.

The temperature of the substrate ranged between 90 and 400 K. It was measured using a thermocouple set in the substrate. For cooling, the substrate was pressed against a copper block, which was cooled by liquid nitrogen. To reach temperatures above room temperature, a resistance heater was inserted in the chamber otherwise used for liquid nitrogen.

To measure the electrical resistance of a thin film we used the four-probe method. The film was 1.7 cm in length and 1-cm wide. At each extremity the film overlapped a gold film to make electrical contacts. On this gold film, thin gold wires were connected by a single-component epoxy Epotek H31. With respect to resistance measurements, let us consider the current I that passes through the film. It must be large enough to permit voltage measurements between two opposite points of the film. But too large a value may involve noticeable changes in the structure of the film by thermal processes. With continuous films, we used the range 10^{-3} A and the error in the resistance measurements was about $\Delta R/R = 10^{-3}$.

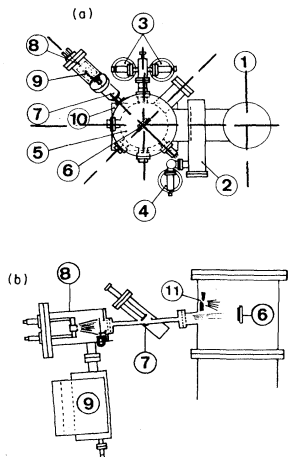


FIG. 1. Diagrams of the experimental arrangement. 1: helium cryopump, 2: ultrahigh-vacuum valve, 3,4: sorption pumps, 5: measurement cell, 6: substrate and sample, 7: ultrahigh-vacuum valve, 8: evaporation chamber, 9: ion pump, 10: ion pump and titanium getter pump, 11: carbon electrodes.

III. EXPERIMENTAL RESULTS

We have checked that the calcium film was not contaminated by residual gases in the cell. It was maintained at low temperature (90 K) under ultrahigh vacuum for about 2 h. Various measurements from time to time after deposition showed that its resistance did not vary with time. Then, if the film was placed under atmospheric pressure, its resistance was increased slowly during a few minutes, and then very quickly. After 15 min the electrical resistance was infinite.

Vacuum-deposited films show a high resistivity compared to that of the bulk. It is well known that annealing decreases generally the resistivity of thin polycrystalline films. This has been attributed¹⁷ to the decrease of the concentration of structural defects. In certain instances, however, heat treatment¹⁸ may lead to an increase in resistivity because of the effect of oxidation and/or agglomeration.

Thus, for calcium films evaporated directly at room temperature, an annealing to 400 K induces an increase in resistivity. We do not try a higher temperature because calcium exhibits a phase transition near¹⁹ 700 K and this effect would be an inconvenience for the electrical measurements. To observe the decrease in resistivity with annealing, the film was prepared at low temperature (90 K); then the temperature was increased to room temperature and then up to 400 K.

The variations of the electrical resistance versus temperature during annealing are shown in Fig. 2. The values of the resistance are taken for each degree, which corresponds to a measure of 45 s for each degree, approximately. With continuous films, the resistance exhibits variations versus temperature that agree with Vand's²⁰ predictions. For sufficiently high temperature, the resistance exhibits a minimum, which is followed by an increase. The latter indicates that the structure of the film has been stabilized, lacunar defects and surface defects being eliminated. Electron photomicrographs were made using the carbon-replica technique.²¹ Before annealing, the surface structure exhibits irregular roughness. After annealing, the surface roughnesses are partially erased (Fig. 3).

After the increase in the resistance has been observed, the film was cooled and a linear decrease of resistance was noted. The uniform decrease is due to the resistivity contribution by thermal vibrations of the lattice, the defect density remaining constant below that of the maximum temperature. During the second cycle of cooling and heating the change

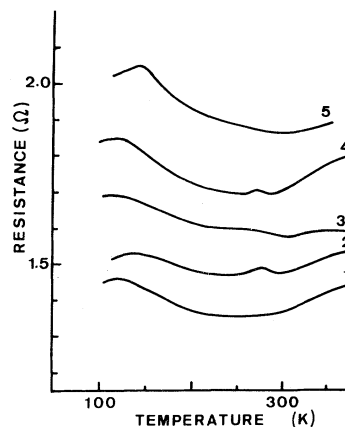


FIG. 2. Variations of the electrical resistance during annealing. The mass thicknesses of the films are, respectively, 1: 132.5 nm, 2: 130 nm, 3: 125 nm, 4: 106 nm, 5: 87.5 nm.

of resistance with temperature is linear (Fig. 4). From electron photomicrographs it can be seen that films with a mass thickness near 30–40 nm have a structure between lacunar and continuous. Hence, the effect of annealing is more important in this case. If the mass thickness is lower, the film structure is lacunar. An increase of the temperature from the cooled substrate temperature involves an increase of the electrical resistance (Fig. 5). Then, a behavior close to reversible is obtained. With continuous films, the slope of the linear variation of the electrical resistivity changes with the film thickness

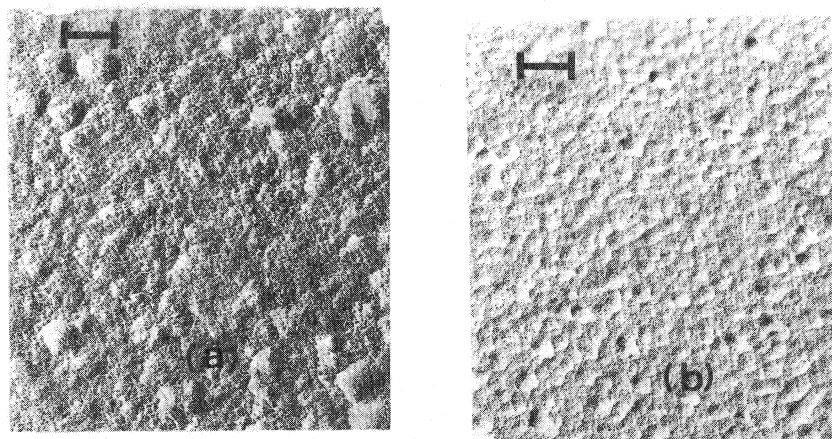


FIG. 3. Electron micrographs of a continuous calcium film (a) before annealing, (b) after annealing. The lines represent 70 nm.

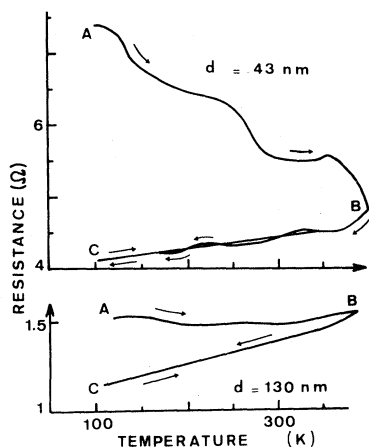


FIG. 4. Electrical resistance plotted against temperature for two continuous films.

(Fig. 6). In spite of a small concavity, linear variations are a good approximation of these curves in the whole range of temperature. The slope of these curves, which was determined between the room-temperature and liquid-nitrogen temperature, increases with the film thickness. It must be emphasized that the resistance versus temperature results found for calcium films are similar to those for many other metals.¹⁷

The electrical resistivity changes with the thickness of the film. These variations can be seen in Fig. 7 for various annealed films (400 K) deposited with the same deposition rate. When the mass thickness is small, the film is discontinuous. Hence, the values of the electrical resistance are great and the conduction is not metallic. It is not our purpose

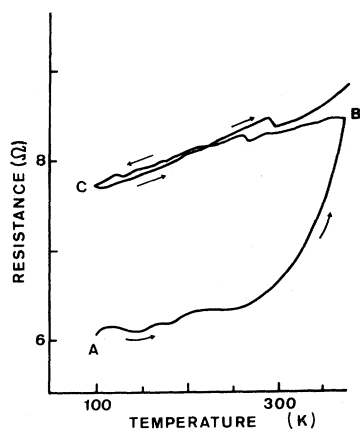


FIG. 5. Electrical resistance plotted against temperature for a lacunar film: $d = 22$ nm.

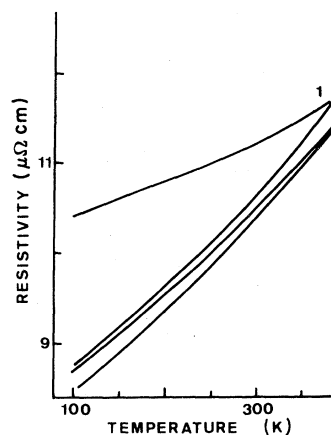


FIG. 6. Electrical resistivity plotted against temperature when the reversible state is reached. The film thicknesses are, respectively, 1: 43 nm, 2: 130 nm, 3: 132.5 nm, 4: 256 nm.

to study a conduction in the present paper. When the mass thickness reaches a value near 30–40 nm, the film structure becomes continuous and the holes can be neglected. With greater values of the thickness the electrical resistivity reaches a constant value. The latter is reached with thicknesses greater than $d_2 \approx 170$ nm, approximately. Then, the electrical resistivity does not depend on thickness, but depends on the film temperature.

IV. DISCUSSION

The first analysis of electrical measurement data for thin films was carried out by Fuchs²² and

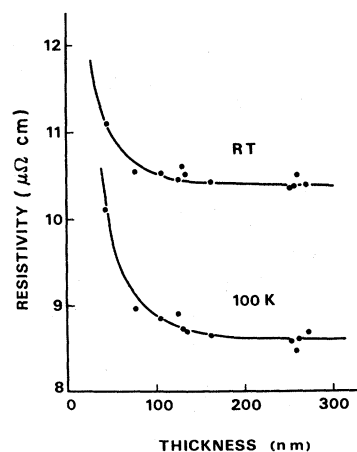


FIG. 7. Electrical resistivity vs film thickness. RT is the curve obtained at room temperature for annealed films. The curve $T = 100$ K was also obtained for annealed films.

developed by Sondheimer,²³ who proceeded from the solution of the Boltzmann equation. In this model, the film is considered of uniform thickness d and limited by plane surfaces, which introduce boundary conditions on the distribution function of the electrons. The general theory assumes that a fraction p of the electrons are reflected specularly at the surfaces while the rest are scattered diffusely. p is supposed to be independent of the direction of motion of electrons and varies between 0 and 1. From the distribution function, the total resistivity of a film is given by

$$\rho_f = \rho_0 \left[1 - \frac{3}{2k}(1-p) \right. \\ \left. \times \int_1^\infty \left[\frac{1}{t^3} - \frac{1}{t^5} \right] \frac{1-e^{-kt}}{1-pe^{-kt}} dt \right]^{-1}, \quad (1)$$

where $k=d/l_0$ is the ratio between the film thickness and the intrinsic mean free path l_0 of the bulk metal, and ρ_0 is the resistivity of the bulk metal.

For thick films, i.e., $k \gg 1$, an approximation of Eq. (1) was given by Sondheimer²³ as follows:

$$\rho_f = \rho_0 \left[1 + \frac{3(1-p)}{8k} \right], \quad (2)$$

and for very large k , a more accurate relation to be used for quick calculations was obtained by Soffer.²⁴

At this stage, if we remember that specular scattering may occur at the two surfaces of the film, the specular parameter p may vary with the nature of the surface. From this assumption Lucas²⁵ introduced two different parameters p and q at the two film surfaces so that Eq. (2) transforms as

$$\rho_f = \rho_0 \left[1 + \frac{3[1 - \frac{1}{2}(p+q)]}{8k} \right]. \quad (3)$$

Although this assumption is reasonable, it is very difficult to separate the influence of each surface of the film on the specular reflection process, and we will use only the parameter p which can represent an averaged value.

The main objections one can find in this theory is that the film approximates a plane-parallel single crystal of metal. In practice this is not the case because evaporated or sputtered films are composed of randomly dispersed polycrystallites and exhibit a rough structure, which is ignored in the Fuchs-Sondheimer (FS) model. Such a structure is shown in Fig. 3.

One of the first attempts to measure the influence of grain boundaries on resistivity was made by Andrews *et al.*,²⁶ who studied polycrystalline copper and aluminum, while the theoretical model was achieved by Mayadas and Shatzkes¹⁴ (MS). In their model, Mayadas and Shatzkes consider the resistivity to be due to isotropic electron scattering (caused by point defects and phonons), to surface scattering (FS effect), and to grain-boundary scattering. These authors started from the assumption that an evaporated or sputtered film is made of grains that grow in a columnlike fashion extending from the substrate to the top of a film (this situation may be observed experimentally for several materials and metals, but we did not see it for calcium). With this hypothesis, grain boundaries are represented by a series of randomly electron-reflecting parallel planes oriented perpendicularly to the film; generally their average distance may be identified with the grain diameter a_g as determined by electron microscope investigations.

For calcium films, which exhibit a great chemical affinity for oxygen and water vapor, we used the carbon-replica technique under ultrahigh vacuum to obtain a replica of unaltered structure. To obtain good contrast and to measure the grain mean height and the grain diameter we used carbon replicas with platinum shadowing at an angle near 70°. From Fig. 3 we measured $a_g \approx 17$ nm after annealing at a temperature near 400 K.

For a polycrystalline film of thickness d , the total resistivity ρ_f including isotropic background scattering, grain-boundary scattering, and external surface scattering has been calculated by Mayadas and Shatzkes¹⁴ as

$$\frac{\rho_f}{\rho_g} = \left[1 - \frac{A}{f(\alpha)} \right]^{-1}, \quad (4)$$

where

$$A = \frac{6}{\pi k}(1-p) \\ \times \int_0^{\pi/2} d\phi \int_1^\infty \frac{\cos^2\phi}{H^2(t,\phi)} \left[\frac{1}{t^3} - \frac{1}{t^5} \right] \\ \times \frac{1 - \exp[-ktH(t,\phi)]}{1-p \exp[-ktH(t,\phi)]} dt, \quad (5)$$

with

$$H(t,\phi) = 1 + \alpha (\cos\phi)^{-1} \left[1 - \frac{1}{t^2} \right]^{-1/2}.$$

ρ_g , which represents the resistivity due to both isotropic background scattering and grain-boundary scattering, is connected to ρ_0 by the relation

$$\rho_g = \frac{\rho_0}{f(\alpha)}, \quad (6)$$

where

$$f(\alpha) = 1 - \frac{3}{2}\alpha + 3\alpha^2 - 3\alpha^3 \ln \left[1 + \frac{1}{\alpha} \right]$$

and

$$\alpha = \frac{l_0}{a_g} \frac{R}{1-R}, \quad (7)$$

R being the grain-boundary reflection coefficient, namely the reflection coefficient of a plane for an electron.

By using the relation (6) the expression (4) transforms as follows:

$$\frac{\rho_f(k, p, \alpha)}{\rho_0} = [f(\alpha) - A]^{-1}. \quad (8)$$

Unfortunately, Eq. (4) and (8) cannot be evaluated analytically but only numerically. As excessively long times are necessary to compute the integrals of (5) by conventional methods, several authors^{27,28} have given numerical tables or an approximate expression for (5) that allow high-speed calculations needed to obtain the particular p and α giving the best fit with experimental data. However, several remarks may help to reduce fitting time. The first one concerns the estimate of p and deals with previous work on the resistivity of polycrystalline films. It is generally shown that the best fit between experiments and the MS model is obtained for p ranging between 0 and 0.5 with the most frequent value $p=0$.

The second remark concerns α . It can be seen from relation (6) that the value of α can be deduced from the knowledge of ρ_g . Mola and Heras²⁷ have shown that the general equations of the Mayadas and Shatzkes theory (MS theory) can be approximated by

$$\rho_f d = \rho_g [d + N(p, \alpha) l_0], \quad (9)$$

where ρ_g , defined earlier can also represent the resistivity of a polycrystalline film of infinite thickness and $N(p, \alpha)$ a numerical function of the two parameters p and α .

Finally, the third remark concerns k . For large k values, it is not necessary to calculate the integrals of (8) for each k . Indeed, very small variations of

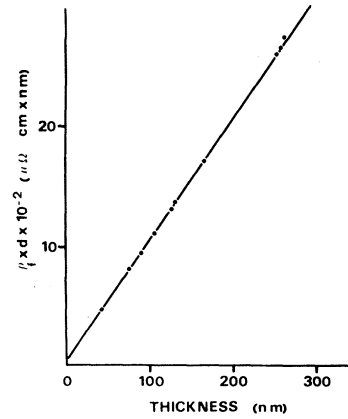


FIG. 8. Variations of the quantity $\rho_f d$ vs d for a series of calcium films at room temperature.

the exponential terms are observed with increasing k so that (8) may be approximated for given α and p by

$$\frac{\rho_f(k, p, \alpha)}{\rho_0} \simeq \frac{1}{f(\alpha)} \left[1 + \frac{1}{k} \left(\frac{1}{\rho_f(1, p, \alpha)/\rho_g} - 1 \right) \right]^{-1}. \quad (10)$$

These equations do not give high accuracy but they enable one to obtain a rapid estimate of the variation of ρ_f/ρ_0 vs k for large k values when a pair (p, α) has been found.

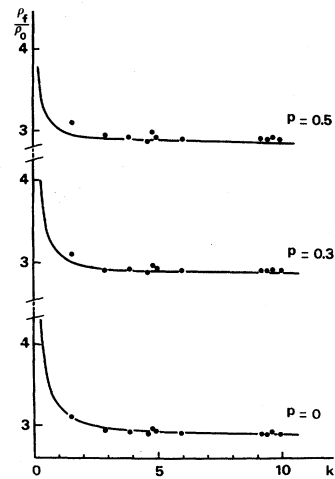


FIG. 9. Fit of experimental data on calcium films to the MS model at room temperature. Network obtained for $\alpha=1.36$ and various p values. ● indicates experimental results.

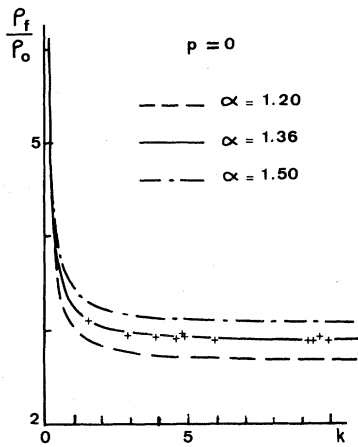


FIG. 10. Fit of experimental data on calcium films to the MS model. Network obtained for $p=0$ and various α , at room temperature.

From the slope of the experimental curve shown in Fig. 8 we found at room temperature $\rho_g = 10.30 \mu\Omega \text{ cm}$ and then $\alpha = 1.36$. As previously indicated this value of ρ_g can represent the limiting resistivity of thick films.

Using various α and p values and with the help of a computer we directly calculated Eqs. (4) and (8) for Ca. The results of these calculations are shown in Figs. 9 and 10 and compared with experimental data. In these plots the k values are equal to the film thickness divided by the electron mean free

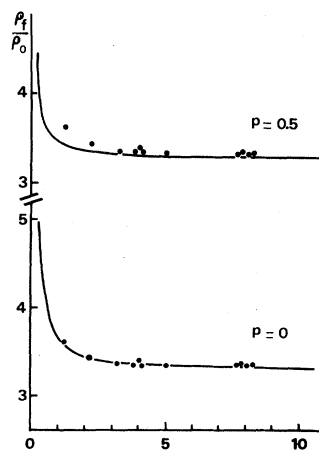


FIG. 11. Fit of experimental data on calcium films to the MS model at 250 K. Network obtained for $\alpha = 1.68$ and various p values. ● indicates experimental results.

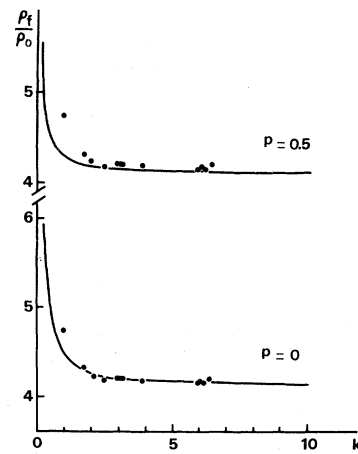


FIG. 12. Fit of experimental data on calcium films to the MS model at 200 K. Network obtained for $\alpha = 2.29$ and various p values. ● indicates experimental results.

path. It is evident that the comparison of experimental curves with theoretical ones needs the knowledge of the mean free path l_0 . The determination of l_0 was obtained in the following way.

We assume in a first approximation that the number of free electrons per atom is taken to be equal to the valence of the metal. The value of $\rho_0 l_0$ is then calculated from the equation

$$\frac{1}{\rho_0 l_0} = \frac{e^2}{\hbar} \left(\frac{n^2}{3\pi^2} \right)^{1/3} \quad (11)$$

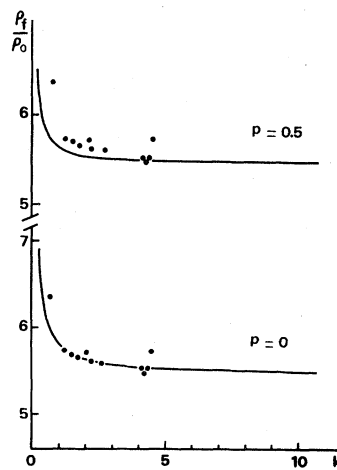


FIG. 13. Fit of experimental data on calcium films to the MS model at 150 K. Network obtained for $\alpha = 3.3$ and various p values. ● indicates experimental results.

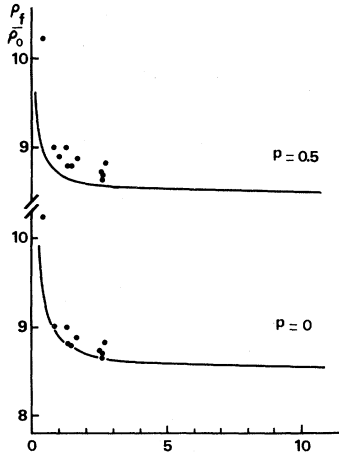


FIG. 14. Fit of experimental data on calcium films to the MS model at 100 K. Network obtained for $\alpha=5.6$ and various p values. ● indicates experimental results.

As $\rho_0=3.6 \mu\Omega \text{ cm}$ for Ca,²⁹ we deduce $l_0=27.2 \text{ nm}$. This procedure is expected to give at least a semiquantitative description of the conduction phenomenon in polycrystalline Ca films.

It can be seen in Fig. 9 that for thick films the ρ_f/ρ_0 values are practically equal to the thick-film limiting value. In a large range of thicknesses, Eq. (8) is not very sensitive to the variations of p between 0 and 0.5; however, numerical theoretical values for ρ_f/ρ_0 decrease with increasing p . For thinner films, a concavity is observed on the curves; in these regions the sensitivity to the p value enables one to find the best fit between theory and experiment.

At room temperature the experimental determination of the p value based on the MS theory is particularly difficult. Looking at Fig. 9, it seems

that the value determined for p depends almost entirely on a single experimental point. To define this value more accurately, we have conducted studies towards lower temperatures. With such conditions the mean free path l_0 increases and the k value decreases for a given film. The various results reported in Figs. 11–14 show that the best fit between experiment and theory is obtained for $p=0$. The results indicate that even if specular reflections occur in thin continuous polycrystalline Ca films, their contribution to the total resistivity is insignificant.

With p value obtained in this way, it is then possible to deduce the mean free path l_0 using the MS theory. Indeed, for two different films prepared under the same conditions we can write

$$\frac{\rho_f(k_1, p, \alpha)}{\rho_0} = [f(\alpha) - A(k_1, \alpha, p)]^{-1} \quad (12)$$

and

$$\frac{\rho_f(k_2, p, \alpha)}{\rho_0} = [f(\alpha) - A(k_2, \alpha, p)]^{-1}, \quad (13)$$

if we assume that the values for α , p , and ρ_0 are thickness independent. Then

$$\frac{\rho_f(k_1, p, \alpha)}{\rho_f(k_2, p, \alpha)} = \frac{f(\alpha) - A(k_2, p, \alpha)}{f(\alpha) - A(k_1, p, \alpha)} \quad (14)$$

and

$$\frac{d_1}{d_2} = \frac{k_1}{k_2}. \quad (15)$$

With the values of $\rho_f(k_1, p, \alpha)/\rho_f(k_2, p, \alpha)$ and d_1/d_2 being given from experimental data, we can solve Eqs. (14) and (15), and obtain the exact values of k_1 and k_2 . The mean free path is deduced immediately as follows:

TABLE I. Mean free path l_0 at room temperature calculated from Eqs. (14)–(16).

Thickness d_1 (nm)	Thickness d_2 (nm)	lpm l_0 (nm)	Thickness d_1 (nm)	Thickness d_2 (nm)	lpm l_0 (nm)
43	165.3	27.9	132.5	165.3	31.5
43	251	27.7	132.5	251	30.8
43	256	28.1	132.5	256	30.1
43	125	30.7	165.3	251	30.2
43	132.5	27.6	165.3	256	29.5
43	105.5	32.2	74.5	25	32.1
74.5	165.3	33	251	256	27.3
74.5	251	32.3			

$$l_0 = \frac{d_1}{k_1} = \frac{d_2}{k_2}. \quad (16)$$

Equation (15) shows that the accuracy of the method to get l_0 needs precise measurements of the thicknesses d_1 and d_2 .

We have solved Eqs. (14) and (15) with a computer. The results of our calculations are reported in Table I for fifteen pairs of films. It can be seen that the averaged value of the electron mean free path l_0 obtained from our experimental data is $l_0 = 30.1 \pm 2.9$ nm. We must note that the use of the approximate equation (9) gives $l_0 = 26.9$ nm.

Now, it is important to examine the influence of grain boundaries on the total resistivity. To solve this question, attention has been paid to the relative dimension between the grain size and the mean free path l due to other scatterers. In particular, it is well known that if the grain size becomes comparable to the mean free path, the grain-boundary scattering may produce a deviation from the Matthiessen's rule, i.e., ρ_g cannot be expressed as the sum of a resistivity ρ_{gb} due to grain boundaries and ρ_0 due to the background. However, according to MS (Ref. 13) and Pichard *et al.*³⁰ this deviation is lower than 5% and a good approximation for ρ_{gb} is as follows:

$$\rho_{gb} = \rho_g - \rho_0. \quad (17)$$

Using $\rho_0 = 3.6 \mu\Omega \text{ cm}$ for calcium, we found $\rho_{gb} = 6.70 \mu\Omega \text{ cm}$. Another expression of ρ_{gb} has been found by Guyot³¹ including the Fermi surface S_F of the metal:

$$\rho_{gb} = \frac{12\pi^3 \hbar}{S_F e^2} R \left[\frac{S}{V} \right], \quad (18)$$

where S/V represents the grain-boundary area per unit volume. Usually S/V is taken to be $2.6/a_g$ for normal grains of diameter a_g whereas in films with a columnar structure $S/V = 2/a_g$ as indicated by Gurr.³² If we want to check this model with the MS model, i.e., if we assume a spherical Fermi surface, we have

$$S_F = \frac{12\pi^3 \hbar}{e^2 \rho_0 l_0},$$

and we obtain another expression of ρ_{gb} , i.e.,

$$\rho_{gb} = \rho_0 l_0 R \frac{2.6}{a_g}. \quad (19)$$

At room temperature, with $\rho_0 = 3.6 \mu\Omega \text{ cm}$, $l_0 = 27.2$ nm, $a_g = 17$ nm, and $R = 0.46$ [this value was deduced from Eq. (7) with $\alpha = 1.36$] Eq. (19)

gives for calcium $\rho_{gb} = 6.89 \mu\Omega \text{ cm}$. The deviation with the first value of ρ_{gb} is lower than 3%. It simply means that at room temperature the approximate value $S/V = 2.6/a_g$ remains valid for Ca which does not exhibit a spherical Fermi surface at all, as shown by Altmann and Craknell.³³ For other temperatures, the values of ρ_{gb} calculated from Eqs. (17) or (19) are given by Table II.

V. CONCLUSION

Thin calcium films have been obtained under ultrahigh vacuum by thermal evaporation onto a cooled substrate. Generally, films contain many structural defects. By applying a relatively mild heat treatment some of these defects disappear. This leads to a corresponding decrease in the film resistivity. For each film, the variations of its resistance versus temperature agree with Vand's predictions.

With the thickest deposits the resistivity reaches a constant value ρ_g that no longer depends on the thickness, but depends on the film temperature. To explain the high value observed for ρ_g , we have used the conduction model proposed by Mayadas and Schatzkes that includes grain boundary scattering. We have shown that the contribution of specular scattering to resistivity is not significant, whereas diffuse scattering occurs for 100, 150, 200, 250, and 300 K. From the knowledge of the parameters p and α , we have deduced the mean free path for polycrystalline films. To find the grain-boundary scattering contribution to the resistivity we calculated the grain-boundary resistivity ρ_{gb} by means of the formula of Guyot or Matthiessen's rule. The values of ρ_{gb} so found is of order of twice the value of the resistivity of the bulk material.

Another electrical quantity of importance is the temperature coefficient of resistivity (TCR) namely,

$$\beta_f = \frac{1}{\rho_f} \frac{\partial \rho_f}{\partial T}.$$

TABLE II. Grain-boundary resistivity ρ_{gb} at various temperatures derived from Eqs. (17) and (19), respectively.

T_K	ρ_{gb} [Eq. (17)] ($\mu\Omega \text{ cm}$)	ρ_{gb} [Eq. (19)] ($\mu\Omega \text{ cm}$)
100	7.44	7.34
150	7.27	7.22
200	7.15	7.16
250	6.90	6.98

This parameter is expected to be different for a thin film and the bulk material. In the past, various attempts³⁴⁻³⁶ have been made to obtain the bulk value β_0 from the TCR β_g of an infinite polycryst-

alline film. A review of the different models used for this purpose and a new one, giving the best fit with calcium data, will be developed in the near future.

-
- ¹P. Rouard, *Thin Solid Films* **34**, 303 (1976).
²P. J. Vernier, *Thin Solid Films* **36**, 223 (1976).
³G. Rasigni, J. P. Palmari, and M. Rasigni, *Phys. Rev. B* **12**, 1121 (1975).
⁴H. Steffen and H. Mayer, *Z. Phys.* **254**, 250 (1972).
⁵P. Gadenne and G. Vuye, *J. Phys. E* **10**, 733 (1977).
⁶O. Hunderi, *J. Phys. F* **6**, 1223 (1976).
⁷J. Marfaing and R. Rivoira, *Phys. Rev. B* **15**, 745 (1977).
⁸P. O. Nilsson and G. Forssell, *Phys. Rev. B* **16**, 3352 (1977).
⁹L. Gaudart and R. Rivoira, *Appl. Opt.* **10**, 2336 (1971).
¹⁰K. A. Kress and G. J. Lapeyre, *Solid State Commun.* **9**, 827 (1971).
¹¹D. J. Mickish, A. B. Kunz, and S. T. Pantelides, *Phys. Rev. B* **10**, 1369 (1974).
¹²C. Lopez-Rios and C. B. Sommers, *Phys. Rev. B* **12**, 2181 (1975).
¹³K. J. Dunn and F. P. Bundy, *Phys. Rev. B* **24**, 1643 (1981).
¹⁴A. F. Mayadas and Shatzkes, *Phys. Rev. B* **1**, 1382 (1970).
¹⁵G. Rasigni, J. P. Palmari, and M. Rasigni, *Surf. Sci.* **50**, 229 (1975).
¹⁶B. V. Bondarenko and V. I. Makhov, *Fiz. Tverd. Tela (Leningrad)* **12**, 1912 (1970) [*Sov. Phys.—Solid State* **12**, 1522 (1971)].
¹⁷K. L. Chopra, *Thin Film Phenomena* (McGraw-Hill, New York, 1969), Chap. 6.
¹⁸D. C. Larson, *Phys. Thin Films* **6**, 81 (1971).
¹⁹J. Katerberg, S. Niemayer, D. Penning, and J. B. Van Zytveld, *J. Phys. F* **5**, L74 (1975).
²⁰V. Vand, *Proc. Phys. Soc. London* **55**, 222 (1943).
²¹L. Gaudart, P. Renucci, and R. Rivoira, *J. Appl. Phys.* **49**, 4105 (1978).
²²K. Fuchs, *Proc. Cambridge Philos. Soc.* **34**, 100 (1938).
²³E. H. Sondheimer, *Adv. Phys.* **1**, 8 (1952).
²⁴S. Soffer, *J. Appl. Phys.* **36**, 3947 (1965).
²⁵M. S. P. Lucas, *Appl. Phys. Lett.* **4**, 73 (1964).
²⁶P. V. Andrews, M. B. West, and C. R. Robeson, *Philos. Mag.* **19**, 887 (1969).
²⁷E. E. Mola and J. M. Heras, *Electrocomp. Sci. Technol.* **1**, 77 (1974).
²⁸C. R. Tellier and A. J. Tosser, *Thin Solid Films* **33**, L19 (1976).
²⁹F. X. Kayser and S. D. Soderquist, *J. Phys. Chem. Solids* **28**, 2343 (1967).
³⁰C. R. Pichard, C. R. Tellier, and A. J. Tosser, *Phys. Status Solidi B* **99**, 353 (1980).
³¹P. Guyot, *Phys. Status Solidi* **38**, 409 (1970).
³²G. J. Van Gurp, *J. Appl. Phys.* **46**, 1922 (1975).
³³S. L. Altmann and A. P. Cracknell, *Proc. Phys. Soc. London* **84**, 761 (1964).
³⁴E. E. Mola and J. M. Heras, *Thin Solid Films* **18**, 137 (1973).
³⁵F. Warkusz, *J. Phys. D* **11**, 689 (1978).
³⁶C. R. Tellier and A. J. Tosser, *Thin Solid Films* **43**, 261 (1977); **44**, 141 (1977); **46**, 307 (1977).

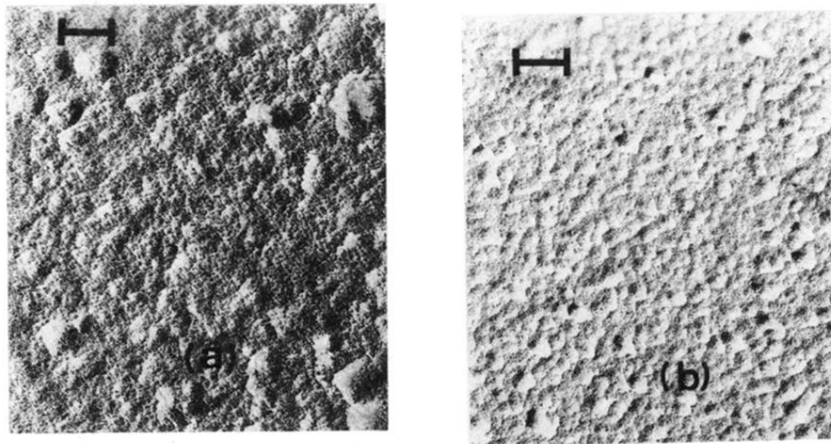


FIG. 3. Electron micrographs of a continuous calcium film (a) before annealing, (b) after annealing. The lines represent 70 nm.